

Monte Carlo simulation study of simple two-dimensional systems

Mike Hughes

(Dated: October 27, 2009)

Abstract

The relationship between the two-particle interaction potential in a system and the macroscopic observables that result is a key issue in statistical mechanics. To explore this relationship, we perform Monte Carlo simulations on a variety of two-dimensional systems including a 2-D Ising model, hard disks, and a 2-D Lennard-Jones system. Our results for the Ising model are in agreement with analytic predictions, demonstrating a second-order phase transition between ordered and disordered phases. For hard disks, we were not able to confirm the prediction that there is a phase transition containing a region where the pressure is constant with increasing density, although there is evidence that a solid forms under certain conditions as expected. We are also able to produce a pressure-density plot at a constant temperature for the Lennard-Jones model, which shows some evidence of a phase transition from a fluid to a solid at the expected density. Additionally, we suggest that using the Gibbs ensemble instead of the canonical ensemble may make for an interesting future study of phase coexistence in this system.

I. ISING MODEL

We begin by examining the two-dimensional ferromagnetic Ising model [4] using Monte Carlo techniques. A square lattice of N dipoles is used in which each dipole interacts only with its nearest neighbors. To minimize edge effects, periodic boundary conditions are imposed. The Hamiltonian for this system is given by [4]:

$$E = -J \sum_{\langle ij \rangle=1}^N s_i s_j - \mu H \sum_i^N s_i \quad (1)$$

where $\langle ij \rangle$ denotes a pair of neighboring dipoles, s_i and s_j are their spins, which can either be up ($s_i = +1$) or down ($s_i = -1$) for a two-state dipole, J is the coupling constant, μ is the dipole moment, and H is the external magnetic field. Each pair of neighboring dipoles that are aligned in spin therefore decreases the total energy by J ; each pair with opposing spins likewise raises the energy by J . In an Ising model with N dipoles, there are $4N$ pairs of neighboring dipoles and therefore $4N$ terms in the Hamiltonian. This problem was solved analytically in the case of zero external field by Onsager in 1944 [3] and our results are compared with Onsager's theoretical predictions. Interestingly, Onsager predicted a second-order phase transition, and we aim to replicate this result computationally. The computational tools developed here will be generalized later to consider the thermodynamic properties of fluids.

The lattice begins in some random initial state, and the Metropolis algorithm [2] is used with each Monte Carlo step to determine whether or not to flip each dipole. Each time a dipole flip is considered, the program evaluates the change in the total internal energy of the lattice that would be caused by flipping the dipole:

$$\Delta E = 2Js_i(s_{above} + s_{below} + s_{left} + s_{right}) - H\mu s_i \quad (2)$$

If flipping the dipole is energetically favorable, lowering the total internal energy of the lattice, the algorithm always performs the flip. Otherwise, the flip is sometimes performed, with a probability equal to the ratio of the Boltzmann factors between the two states:

$$P = e^{-\beta\Delta E} \quad (3)$$

Each dipole in the lattice is considered in succession, and the process continues until a predetermined number of Monte Carlo steps have been performed for every dipole in the

lattice. The algorithm samples the total internal energy per dipole and the magnetization per dipole every 1000 Monte Carlo steps, where the internal energy per dipole is simply the Hamiltonian divided by N , and

$$m = \frac{\mu(N_{up} - N_{down})}{N} \quad (4)$$

The mean and standard deviation of these two quantities are taken for the last half of the run (the first half is not considered to reduce the effect of the system starting out far from equilibrium), and the data are compared with theoretical predictions. The energy is reported in units of the interaction energy J and the temperature is input in units of J over Boltzmann's constant k .

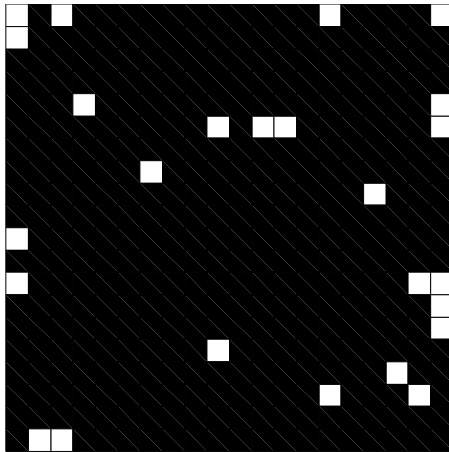


FIG. 1: 20x20 Ising model at $T=2J/k$ after 500 Monte Carlo steps per dipole. White squares represent spin-up dipoles, black squares spin-down ones.

This program was run for temperatures ranging from 1.0 J/k to 3.5 J/k in increments of 0.02 J/k using a 100x100 lattice. At each temperature, 15000 Monte Carlo steps were performed per dipole in the lattice. Results for internal energy and magnetization were obtained and are shown in Fig. 4 and Fig. 3 respectively. Further, as shown below, the

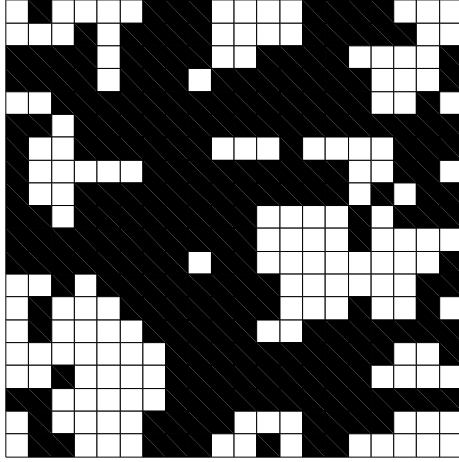


FIG. 2: 20x20 Ising model at $T=3J/k$ after 500 Monte Carlo steps per dipole. Note that, while there is a definite net magnetization at $T=2J/k$, there are now roughly the same number of dipoles pointing up versus down.

specific heat can also be calculated directly from the standard deviation of the internal energy without taking any numerical derivatives.

We start from the definition of the specific heat,

$$c \equiv \frac{1}{N} \frac{\partial E}{\partial T} \quad (5)$$

which can be rewritten using $\beta \equiv \frac{1}{kT}$ as:

$$c = -\frac{\beta^2}{N} \frac{\partial E}{\partial \beta} \quad (6)$$

Note that the average energy (i.e. the internal energy is calculated from the partition function by:

$$\langle E \rangle = -\frac{1}{Z} \frac{\partial Z}{\partial \beta} \quad (7)$$

where Z is the partition function. Combining the two,

$$\frac{\partial \langle E \rangle}{\partial \beta} = -\frac{\partial}{\partial \beta} \left(\frac{1}{Z} \frac{\partial Z}{\partial \beta} \right) = \frac{1}{Z^2} \left(\frac{\partial Z}{\partial \beta} \right)^2 - \frac{1}{Z} \frac{\partial^2 Z}{\partial \beta^2}. \quad (8)$$

Eq. (7) is then used to produce

$$\frac{\partial \langle E \rangle}{\partial \beta} = \langle E^2 \rangle - \langle E \rangle^2 \quad (9)$$

from which we use (6) and $\sigma^2 = \frac{\langle E^2 \rangle - \langle E \rangle^2}{N}$ to produce

$$c = \frac{\sigma^2}{T^2} \quad (10)$$

where σ is the standard deviation in the energy and β has been expressed as $1/T$ (in units where $k = 1$). Hence, the specific heat is calculated directly from the standard deviation of the internal energy without the need to evaluate a numerical derivative via Eq. (6). Our results are then compared to the theoretical predictions given in [4]. Onsager's result for the magnetization per dipole is given by

$$m = \begin{cases} \{1 - [\sinh(2\beta J)]^{-4}\}^{1/8} & T < T_c \\ 0 & T > T_c, \end{cases} \quad (11)$$

while the internal energy per dipole is predicted to be

$$u_I = -J \coth 2\beta J \left[1 + \frac{2}{\pi i} \kappa' K_1(\kappa) \right] \quad (12)$$

where

$$\kappa \equiv \frac{2 \sinh 2\beta J}{\cosh^2 2\beta J} \quad (13)$$

$$\kappa' \equiv 2 \tanh^2 2\beta J - 1 \quad (14)$$

and

$$K_1(\kappa) \equiv \int_0^{\pi/2} \frac{d\phi}{\sqrt{1 - \kappa^2 \sin^2 \phi}} \quad (15)$$

The results obtained here are in good agreement with theory, as evidenced by Figs. 3,4, and 5. The second-order phase transition between ordered and disordered states is expected to occur at $T_c = 2.269J/k$, at which point the average magnetization of the system drops abruptly to zero. Our model shows that a phase transition consistent with this critical temperature does occur, and almost all the data are in agreement with the theoretical predictions. Notably, the phase transition is clearly second-order - the energy is differentiable, but the specific heat certainly is not. There are three notable outliers in the magnetization data for $T < T_c$. The explanation for these lies in the fact that, at sub-critical temperatures, the model can settle into higher-energy metastable states for long periods of time;

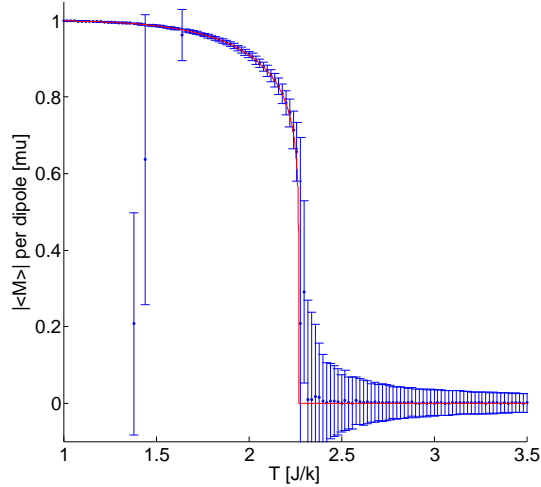


FIG. 3: Average magnetization per dipole. The solid line represents Onsager’s prediction; points with error bars represent Monte Carlo results.

these three evidently had not moved to the lowest-energy state by the time data began to be recorded in the second half of the run, although further analysis suggests that the two points with error bars overlapping the theoretical curve had reached the predicted value by the end of the run. These points show up as outliers in the energy and specific heat curves as well.

A further run was performed to test the effect of non-zero external magnetic fields on the system’s magnetization. As expected, the system responded less strongly to temperatures above the critical point as the external field was increased. Our results, shown in Figure 6, agree with the qualitative graph given in [4].

II. REVIEW OF STATISTICAL MECHANICS FOR FLUIDS

Following the Ising model, we examine systems of fluids with hard disk and Lennard-Jones interactions. To understand these interactions from first principles, a review of statistical

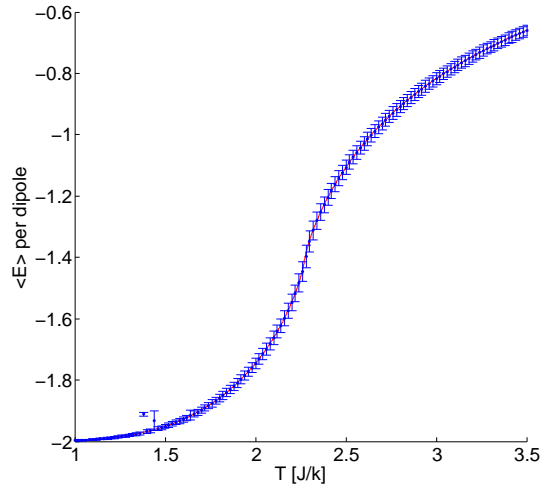


FIG. 4: Average internal energy per dipole. Solid line represents Onsager's prediction, points with error bars represent Monte Carlo results

mechanics for fluids is in order. In particular, we are interested in how to compute the pressure from a given two-particle interaction potential.

We start with the full two-dimensional partition function

$$Z = \frac{1}{h^{2N} N!} \int dp^N dr^N \exp \left(-\beta \left(\sum_i \frac{p_i^2}{2m} + \sum_{i<j} u_{ij} \right) \right) \quad (16)$$

where $dp^N = d\mathbf{p}_1 d\mathbf{p}_2 \dots d\mathbf{p}_N$ and u_{ij} denotes the potential between two particles separated by distance r_{ij} . The kinetic energy part of the integral depends only on momenta p and the potential energy part depends only on positions r . Thus we can factor the integrand, so that we have the product of two integrals:

$$Z = \frac{1}{h^{2N} N!} \int dp^N \exp \left(-\beta \sum_i \frac{p_i^2}{2m} \right) \int dr^N \exp \left(-\beta \sum_{i<j} u_{ij} \right) \quad (17)$$

First we will evaluate the kinetic energy integral. It can be rewritten:

$$\int d\mathbf{p}_1 d\mathbf{p}_2 \dots d\mathbf{p}_N \exp \left(-\beta \sum_i \frac{p_i^2}{2m} \right) \quad (18)$$

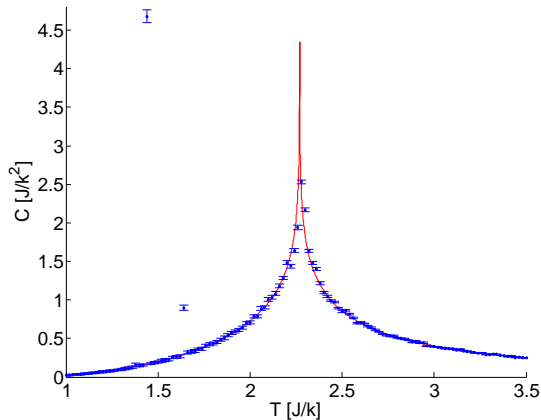


FIG. 5: Specific heat for the Ising model. Solid line represents Onsager's prediction, points with error bars represent Monte Carlo results

$$= \left(\int d\mathbf{p}_1 \exp\left(-\beta \frac{p_1^2}{2m}\right) \right)^N \quad (19)$$

Making the substitution $q = p\sqrt{\frac{2m}{\beta}}$ and doing the integral in polar coordinates, this results in

$$= \left(\int_0^\infty dq 2\pi \left(\sqrt{\frac{2m}{\beta}}\right)^2 \exp(-q^2) \right)^N \quad (20)$$

$$= \left(\frac{4\pi m}{\beta} \int_0^\infty dq q \exp(-q^2) \right)^N \quad (21)$$

This integral can now easily be solved analytically, producing

$$\int dp^N \exp\left(-\beta \sum_i \frac{p_i^2}{2m}\right) = \left(\frac{2\pi m}{\beta}\right)^N \quad (22)$$

The quantity $h/\sqrt{2\pi mkT}$ is called the thermal wavelength, λ_T . Using the above result and substituting in λ_T , we arrive at

$$Z = \frac{1}{N! \lambda_T^{2N}} \int dr^N \exp\left(-\beta \sum_{i<j} u_{ij}\right) \quad (23)$$

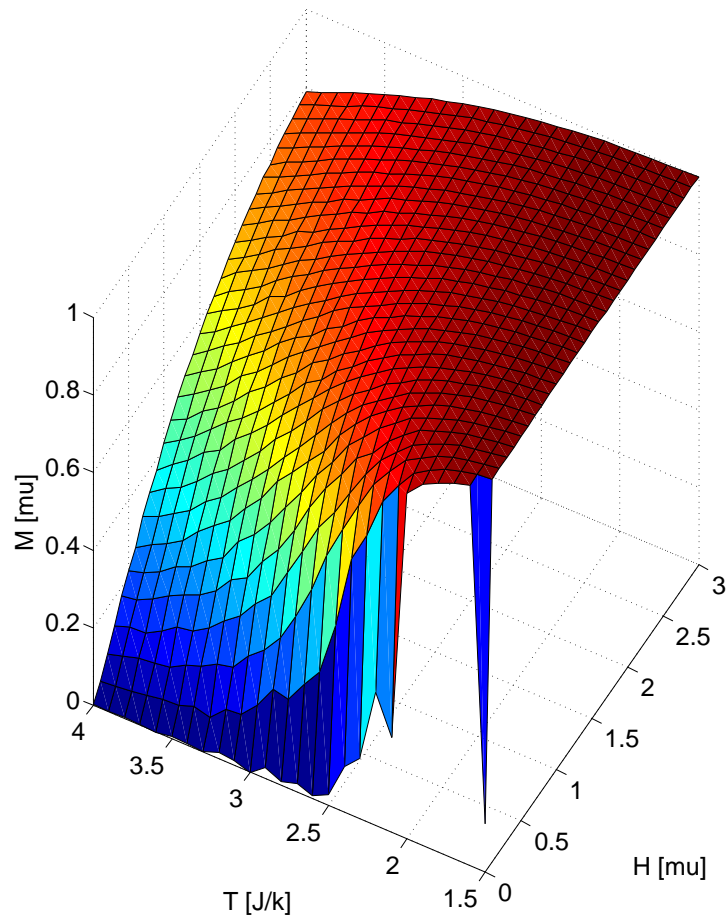


FIG. 6: Plot of Ising model magnetization as a function of external magnetic field H and temperature T

At this point, we are able to invoke the relation $F = -kT \ln Z$, where F is the Helmholtz free energy, and the relation $P = -\frac{\partial F}{\partial V}$. This leads us to

$$\beta P = \frac{\partial}{\partial A} \ln \left(\int dr^N \exp \left(-\beta \sum_{i<j} u_{ij} \right) \right) \quad (24)$$

Then, we change coordinates to $\tilde{r} = A^{-1/2}r$, so that $d\tilde{r} = A^{-1} dr$. Now we have

$$\beta P = \frac{\partial}{\partial A} \ln \left(A^N \int d\tilde{r}^N \exp \left(-\beta \sum_{i<j} u(A^{1/2}\tilde{r}_{ij}) \right) \right) \quad (25)$$

Noting that

$$Q = \ln \left(A^N \int d\tilde{r}^N \exp \left(-\beta \sum_{i<j} u(A^{1/2}\tilde{r}_{ij}) \right) \right) \quad (26)$$

where Q denotes the configurational partition, we take the derivative in (25) and substitute Q into the result, yielding

$$\beta P = \frac{1}{Q} \left(\frac{NQ}{A} + A^N \int d\tilde{r}^N \frac{\partial}{\partial A} \exp \left(-\beta \sum_{i<j} u(A^{1/2} \tilde{r}_{ij}) \right) \right) \quad (27)$$

The first term is simply ρ , the density. Using the chain rule on the second term, we get

$$\beta P = \rho - \frac{\beta A^N}{2Q} \int d\tilde{r}^N \sum_{i<j} \left(A^{-1/2} \tilde{r} \frac{du}{dr} \right) \exp \left(-\beta \sum_{i<j} u(A^{1/2} \tilde{r}_{ij}) \right) \quad (28)$$

There are $N(N-1)/2$ terms in the sum outside the exponential, and they no longer depend on i or j . Thus, without loss of generality, we can state

$$\sum_{i<j} \left(A^{-1/2} \tilde{r} \frac{du}{dr} \right) = \frac{1}{2} N(N-1) A^{-1/2} \tilde{r}_{12} \frac{du_{12}}{dr_{12}} \quad (29)$$

Substituting, and switching coordinates from \tilde{r} back to r , we can express βP as

$$\beta P = \rho - \frac{\beta}{2Q} \int d\mathbf{r}_1 d\mathbf{r}_2 \frac{1}{2} N(N-1) \left(r_{12} \frac{du_{12}}{dr_{12}} \right) \int dr^{N-2} \exp \left(-\beta \sum_{i<j} u(r_{ij}) \right) \quad (30)$$

This now allows us to invoke the relation

$$\rho^2 g(r_1, r_2) = N(N-1) A^{-N} Q^{-1} \int dr^{N-2} \exp \left(-\beta \sum_{i<j} u(r_{ij}) \right) \quad (31)$$

from [8]. Substituting this into Eq. (30), we get the virial theorem for two-body interactions in two dimensions, which is

$$\beta P = \rho - \frac{\beta \rho^2}{4} \int d\mathbf{r} r g(r) \frac{du}{dr} \quad (32)$$

III. HARD DISKS

We next examine two-dimensional systems of hard disks. The hard disk potential is perhaps the simplest pair potential that yields macroscopic properties that deviate from the ideal gas. It is defined as

$$V = \begin{cases} \infty & r < \sigma \\ 0 & r > \sigma \end{cases} \quad (33)$$

where σ is the diameter of each disk.

In other words, the particles are disks that float around freely, except that they are constrained not to overlap with each other. Although temperature does not affect this model's behavior, it is interesting because, as the density is increased, the number of configurations that does not produce overlapping particles gets smaller. At high enough densities, the pair correlation function indicates that the system undergoes a phase transition from a fluid to a solid. [9] finds that this phase transition is marked by a discontinuous change in the pressure as a function of density. We aim to reproduce this finding.

To investigate this, a number N of disks are placed in a square region with periodic boundary conditions. With each pass, a trial displacement is performed on each disk in sequence. The magnitudes of the displacements are decided at random from within a range chosen so that the number of accepted new configurations is about 50% of the number attempted. The pair correlation function $g(r)$ is approximately computed by keeping track of the number of particles n_{ji} that are located between distances r and $r + \delta r$ away from a tagged particle i for pass j . This is performed for each particle in the simulation. A method for determining $g(r)$ from Monte Carlo calculations is provided in [6].

First, a desired resolution δr is specified. $g(r)$ can be determined by averaging the number of occurrences of particular pair separations. Suppose a shell is located between distances r and $r + \delta r$. On some pass j , the algorithm counts the number of particles within this shell for each particle and then averages this over all the particles in the system. Let $\langle n_j(r) \rangle$ be this average for pass j . Then

$$\langle n_j(r) \rangle = \frac{1}{N} \sum_{i=1}^N n_{ji} \quad (34)$$

Then, we average this quantity over the total number of passes P that are performed during the simulation. We call this average $\langle n(r) \rangle$. Thus

$$\langle n(r) \rangle = \frac{1}{P} \sum_{j=1}^P \langle n_j(r) \rangle = \frac{1}{NP} \sum_{j=1}^P \sum_{i=1}^N n_{ji} \quad (35)$$

If the particles' positions were entirely uncorrelated, then $g(r) = 1$ and, for some particle density ρ , $\langle n(r) \rangle_{unc} = (\text{area of shell})\rho(N - 1)/N$. The factor of $(N - 1)/N$ corrects for the fact that tagged particles cannot be within their own shells. $g(r)$ can then be expressed as $\frac{\langle n(r) \rangle}{\langle n(r) \rangle_{unc}}$, and the shell's area is $\pi\delta r(2r + \delta r)$, so

$$g(r) = \frac{\sum_{i=1}^N \sum_{j=1}^P n_{ji}(r)}{\pi P \rho \delta r (2r + \delta r) (N - 1)} \quad (36)$$

From the pair correlation function, we can use the virial theorem Eq. (??) to compute the pressure. The virial theorem in two dimensions is

$$P = \frac{\rho}{\beta} - \frac{\rho^2}{4} \int d\mathbf{r} r \frac{dV}{dr} g(r) \quad (37)$$

Note that the original 1/6 from [8] is replaced with 1/4 appropriate for a two-dimensional system. In order to calculate the pressure for hard disks, we first differentiate the Boltzmann factor to find that

$$\frac{d}{dr}(e^{-\beta V}) = -\beta e^{-\beta V} \frac{dV}{dr} \quad (38)$$

Rearranging,

$$\frac{dV}{dr} = -\frac{1}{\beta} e^{\beta V} \frac{d}{dr}(e^{-\beta V}) \quad (39)$$

We also note that, for hard disks, $e^{-\beta V}$ is simply a step function $\theta(r - \sigma)$: its value is 1 for $r > \sigma$ and 0 for $r < \sigma$. The derivative of a step function is a Dirac delta function, so $\frac{d}{dr}(e^{-\beta V}) = \delta(r - \sigma)$. Inserting this into (39), we find

$$\frac{dV}{dr} = -\frac{1}{\beta} e^{\beta V} \delta(r - \sigma) \quad (40)$$

This is then inserted into (32), producing

$$P = \frac{\rho}{\beta} + \frac{\rho^2}{4} \int d\mathbf{r} \frac{r}{\beta} e^{\beta V} \delta(r - \sigma) g(r) \quad (41)$$

which is equivalent to

$$P = \frac{\rho}{\beta} + \frac{\pi \rho^2}{2\beta} \int r^2 e^{\beta V} \delta(r - \sigma) g(r) dr \quad (42)$$

Evaluating this integral from the right, we see that

$$P = \frac{\rho}{\beta} + \frac{\pi \rho^2 \sigma^2}{2\beta} g(\sigma^+) \quad (43)$$

in agreement with the result in the discussion of Monte Carlo simulations of hard disk fluids in [6] (Problem 7.33).

A simulation with $N = 144$ was performed for reduced densities $\rho^* \equiv \rho \sigma^2$ ranging from $\rho^* = 0.79$ to $\rho^* = 0.85$. Alder and Wainwright [9] predict a first-order phase transition

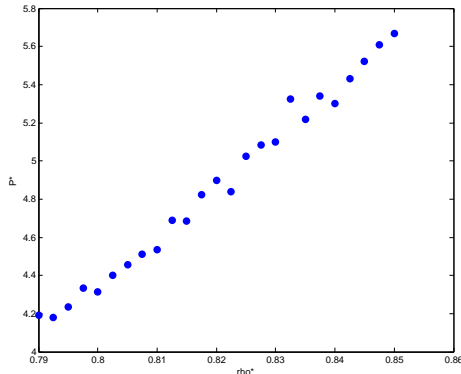


FIG. 7: Pressure versus density graph for hard disks

between fluid and solid phases to occur, with phase coexistence between pure fluid and pure solid for a range of reduced densities between 0.81 and 0.85, in which range the pressure should be constant. Our observations, shown in Fig. 9, did not confirm this. Our simulations show the pressure increases almost monotonically, with some minor fluctuations that are most likely caused by the inherent randomness of Monte Carlo simulations. A broader simulation for reduced densities between 0.3 and 0.9 likewise showed steadily increasing pressure. The correlation function does show oscillations around $g(r) = 1$ that fall off heavily for lower densities but are more pronounced for higher densities. At sufficiently high densities, it displays behavior that is indicative of a periodic crystal structure, so there is evidence that a solid does form, albeit without a van der Waals-like phase transition.

IV. LENNARD-JONES POTENTIAL IN TWO DIMENSIONS

We next move on to a slightly more complicated potential, the Lennard-Jones potential. It is defined as

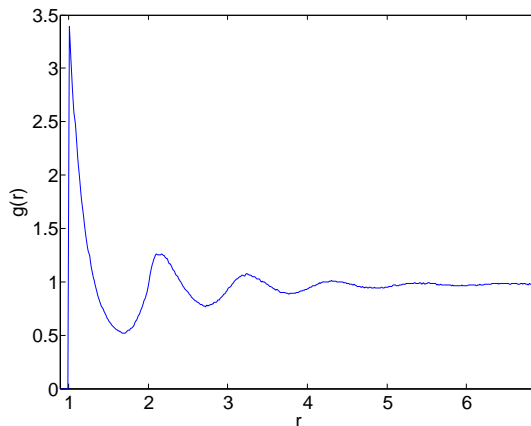


FIG. 8: Hard disk pair correlation function for $\rho^* = 0.74$. Note that $g(r)$ oscillates smoothly and that it goes to 1 rapidly; this is indicative of a dense fluid.

$$V = 4\epsilon \left(\left(\frac{\sigma}{r} \right)^{12} - \left(\frac{\sigma}{r} \right)^6 \right) \quad (44)$$

The Lennard-Jones model simulates the behavior of noble gas atoms. It is qualitatively similar to the hard disk model for $r < \sigma$ in that the potential climbs very rapidly if two particles begin to overlap, as one would expect. Unlike the hard disk model, there is a long-range attractive potential between particles for $r > \sigma$. One can show that the minimum of the potential well is at $r = 2^{1/6}\sigma = 1.12\sigma$. Thus, we would expect that the particles will prefer to clump together at about this distance away from each other at low temperatures.

The Lennard-Jones potential is simulated under similar conditions as the hard disk model: a square region with periodic boundary conditions is used to hold N particles. The distance from each particle to each other particle is computed and stored in a matrix. The Lennard-Jones potential is applied to each entry in the matrix and all the entries are summed to produce the internal energy of the system. As with the hard disks, with every pass, an attempt is made to move each particle in sequence. Each time a new configuration is

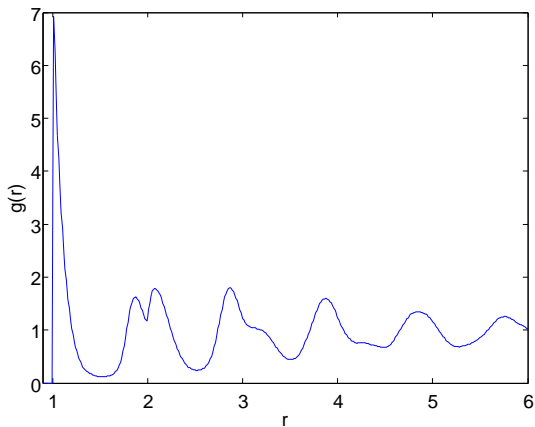


FIG. 9: Pair correlation function for hard disks with $\rho^* = 0.95$. Here, $g(r)$ has noticeable secondary peaks and does not approach 1 rapidly, which indicates that a periodic structure and hence a solid has formed

generated, the internal energy of this configuration is calculated and compared with the old internal energy. As with the Ising model, the new configuration is always accepted if it has a lower internal energy than the old configuration, and it is sometimes accepted, with a probability equal to the ratio of the Boltzmann factors of the new state to the old (see Eq. (3)), if the new configuration has a higher energy.

Because each attempted configuration requires us to recalculate the distance from the displaced particle to every other particle in the simulation and then apply the Lennard-Jones potential to determine the new internal energy, these simulations are computationally intensive. It is common to truncate the Lennard-Jones potential beyond a certain distance, commonly 2.5σ , to save time. However, Smit and Frenkel [10] determined that truncation of the Lennard-Jones potential causes significant differences in the results even though it may appear that the potential is negligibly small past some cutoff value. Therefore, we use the full potential, at the cost of running long simulations.

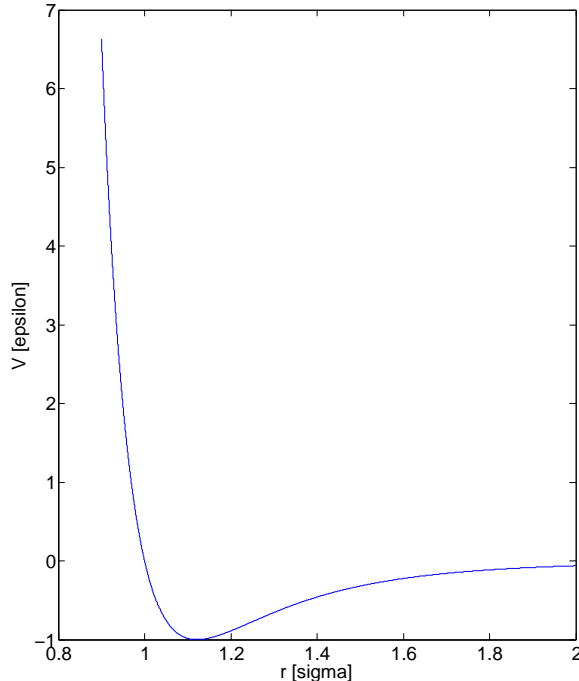


FIG. 10: The Lennard-Jones potential

Barker et al. [7] find a phase diagram that is qualitatively similar to the three-dimensional situation, with distinct solid, liquid, and gas phases and a critical point after which the two fluid phases become indistinguishable. Because of time constraints, we could not attempt to verify the entire phase diagram, but we did plot the pressure-density isotherm at $T^*=0.7$ to see if a noticeable phase transition between fluid and solid phases predicted to occur near $\rho^* = 0.8$.

We performed a run at $T^*=0.7$ between $\rho^* = 0.7$ and $\rho^* = 0.9$ for $N=144$ disks, completing 10000 passes per density increment. The first 2000 passes are discarded to allow the system to approach equilibrium; using the remaining data, $g(r)$ is computed in the same manner as it is for hard disks (see Eq. (36)). The pressure is then computed from the virial theorem Eq. (37). Bode's eight-point rule [11] is used to perform the necessary numerical integration.

The results of this run are shown in Figure 11. Our results agree with Barker et al. in that the pressure does fall slightly as density increases and the system freezes around $\rho = 0.82$, so there does appear to be a phase transition here. Other interesting observables we would

like to calculate in future work are the heat-capacity and isothermal compressibility.

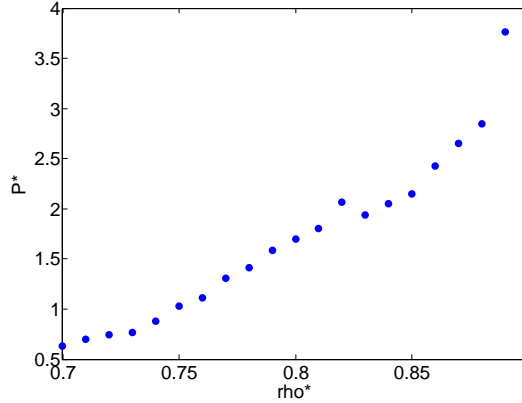


FIG. 11: Pressure-density graph for Lennard-Jones simulation at $T^*=0.7$

V. GIBBS ENSEMBLE

In addition to the canonical ensemble, we also explore the Gibbs ensemble, which enables phase coexistence properties to be calculated without fixing the density by assuring phase equilibrium between two coupled regions. Panagiotopoulos [5] gives an algorithm to perform calculations in the Gibbs ensemble for three-dimensional fluids, which can easily be modified for two dimensions. The system consists of two initially identical regions in a square box containing a total of N particles. Periodic boundary conditions are imposed, and the algorithm proceeds in three steps. For all three steps, the probability of acceptance is given by the ratio of the Boltzmann factor of the new state to that of the old state, if the new state has a higher energy, and is 1 otherwise (see Eq. (3)). In the first, trial displacements are attempted on each side, totaling N attempted displacements. Each displacement attempt is performed on a random particle, a random direction is chosen, and a random distance is

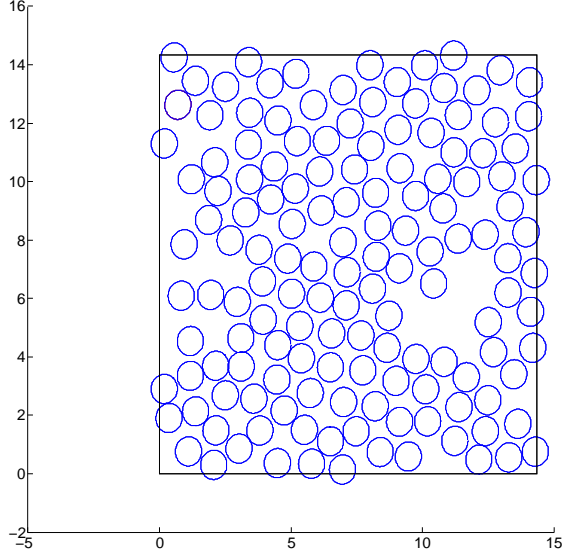


FIG. 12: One sample Lennard-Jones configuration at $\rho^* = 0.7$

picked from a uniformly distributed range, selected to produce an acceptance rate of about 50%. Then, a single attempt to change the volume is performed. In this step, one region is increased in volume by some randomly chosen amount and the other side has its volume decreased by the same amount, so that the total volume stays constant. The energy change due to a change in volume ΔV of region I is

$$\Delta E = \Delta E^I + \Delta E^{II} - N^I kT \ln \frac{V^I + \Delta V}{V^I} - N^{II} kT \ln \frac{V^{II} - \Delta V}{V^{II}} \quad (45)$$

where the last two terms come from the ideal gas contribution to the change in entropy. They are included to keep the regions at constant temperature. [5]

The third step involves moving random particles from one region to random positions in the other. The number of these steps is capped at 2% of N ; Panagiotopoulos [5] notes that erroneous results for the pressure may be obtained if this number is much higher. Each particle exchange from region I to region II changes the energy by

$$\Delta E = \Delta E^I + \Delta E^{II} + N^I kT \ln \frac{N^I + 1}{N^I} + N^{II} kT \ln \frac{N^{II} - 1}{N^{II}} + kT \ln \frac{V^{II}}{N^{II} - 1} - kT \ln \frac{V^I}{N^I + 1} \quad (46)$$

where in this case the logarithmic terms in the energy change exist to hold the chemical potential constant. [5]

Although a working Gibbs ensemble code was produced, we were not able to produce many results due to time constraints. It would be interesting to use the Gibbs ensemble to explore phase coexistence with the Lennard-Jones and other potentials. This could be a good avenue for further study.

-
- [1] S. Kadlec. *Phase Equilibrium in Various Systems of Hard and Soft Core Particles*. Ph. D. thesis, University of Colorado, 2004.
 - [2] N. Metropolis et al. Equation of state calculations by fast computing machines. *J. Chem. Phys.*, **21**:1087, 1953.
 - [3] L. Onsager. Crystal Statistics. I. A Two-Dimensional Model with an Order-Disorder Transition. *Phys. Rev. Lett.*, **65**:117, pp. 117-149.
 - [4] K. Huang. *Statistical Mechanics*. John Wiley and Sons, 1987.
 - [5] A. Z. Panagiotopoulos. Direct determination of phase coexistence properties of fluids by Monte Carlo simulation in a new ensemble. *Molecular Physics*, **61**:527, 1987.
 - [6] D. Chandler. *Introduction to Modern Statistical Mechanics*. Oxford University Press, 1987.
 - [7] J.A. Barker et al. Phase diagram of the two-dimensional Lennard-Jones system; evidence for first-order transitions. *Physica* 106A, pp. 226-238, 1981.
 - [8] R. Balescu. *Equilibrium and Nonequilibrium Statistical Mechanics*. John Wiley and Sons, 1975.
 - [9] B. J. Alder and T. E. Wainwright. Phase transition in elastic disks. *Physical Review*, **127**:359, 1962.
 - [10] B. Smit and D. Frenkel. Vapor-liquid equilibria of the two-dimensional Lennard-Jones fluid(s). *J. Chem. Phys.*, **94**:5663, 1991.
 - [11] M. Abramowitz and I. A. Stegun. *Handbook of mathematical functions*. Dover Publications, 1972.
 - [12] D. Schroeder. *An Introduction to Thermal Physics*. Addison Wesley Longman, 2000.